The International Archives of the Photogrammetry, Remote Sensing and Spatial Information Sciences, Volume XLIII-B2-2022
XXIV ISPRS Congress (2022 edition), 6–11 June 2022, Nice, France

COMBINING UNMANNED AERIAL SYSTEMS AND STRUCTURE FROM MOTION PHOTOGRAMMETRY TO RECONSTRUCT THE GEOMETRY OF GROINS

D. Gonçalves [1,2*], G. Gonçalves [1,3], J. Pérez-Alvárez [4], M. C. Cunha [2], U. Andriolo [1]

[1] INESC Coimbra, Dept. of Electrical and Computer Engineering, Polo 2, 3030-290 Coimbra, Portugal - (diogo.goncalves, uandriolo)@mat.uc.pt

[2] Dept. of Civil Engineering, University of Coimbra, 3030-788 Coimbra, Portugal - mccunha@dec.uc.pt

[3] Dept. of Mathematics, University of Coimbra, 3001-501 Coimbra, Portugal - gil@mat.uc.pt

[4] Graphic Expression Dept., University Centre of Merida (CUM), University of Extremadura, 06800 Badajoz, Spain - japerez@unex.es

Commission II, WG II/10

KEY WORDS: drones, coastal engineering, survey, Structure from Motion, Digital Surface Model, monitoring

ABSTRACT:

In the context of coastal environment, the combined use of Unmanned Aerial Systems (UAS) with Structure-from-Motion (SfM) photogrammetry has been demonstrated to be a suitable tool to collect accurate geoinformation. This work aims at investigating the effectiveness of UAS survey to accurately map the geometry of rouble mound groins for monitoring the structural integrity. A set of nadiral images was processed through SfM photogrammetry to obtain the Digital Surface Model (DSM) of the groin. The DSM accuracy was evaluated through the comparison of five profiles measured by the traditional GNSS technique. Overall, vertical accuracy returned a root mean square error of 2.6 cm. The results suggest that UAS combined with SfM photogrammetry can improve the current monitoring of coastal engineering structures by providing high accurate geospatial products.

1. INTRODUCTION

The coastal environment is the high dynamic interface between land and ocean. In the last decades, remote sensing techniques have been used for monitoring coastal environments (Andriolo et al., 2018; Laporte-Fauret et al., 2020; Mancini et al., 2013; Medjkane et al., 2018; Turner et al., 2016; Zimmerman et al., 2020) Among these, Unmanned Aerial Systems (UAS) allow to acquire images with high resolution to 3D reconstruct the geometry and to potentially increase the survey frequency of coastal features. UAS have been used for monitoring beach and dunes (Bañón et al., 2019; Pagán et al., 2019; Rotnicka et al., 2020), morphological change in cliffs (Gómez-Gutiérrez and Gonçalves, 2020; Ružić et al., 2014), mapping marine litter (Andriolo et al., 2021, 2020; Duarte et al., 2020) and vegetation classification (Laporte-Fauret et al., 2020).

Among coastal engineering structures, groins are built shore perpendicular to maintain updrift beaches, or to restrict longshore sediment transport (CIRIA et al., 2007). The armour layer is the groin section that protects the structure from wave attacks and storms. It is usually composed of stone blocks and/or concrete (Bush et al., 2001). The structural condition of armour layer represents the assessment of structural integrity (CIRIA et al., 2007), and consequently the assessment of likely movements in armour layer units inducted by waves and/or storms. Therefore, preserving the integrity of the structure is fundamental to preserve the safety of coastal communities.

In this context, the monitoring of groins should be repeatable over time. There are four levels of surveys to evaluate the condition of armour units (CIRIA et al., 2007): (1) locating armour units movements measuring with Global Navigation Satellite System (GNSS) surveys; (2) geometric survey to describe armour layer with similar techniques of level 1; (3) armour units position including voids and areas (photographic methods such as photogrammetry or comparative photography); (4) shape and size of armour units including armour fractures.

Nowadays, the monitoring of groins and breakwaters is mainly done by visual inspection. Trained technicians walk through the structure to identify likely armour layer movements. This technique lacks accurate geospatial information and temporal resolution. In several cases, the likely damaged areas are almost impossible to reach due to its location in the wave breaking zone which compromises the safety of technicians (Henriques et al., 2017).

The 3D reconstruction of surfaces from a UAS-based imagery survey can be a potential solution for monitoring groins and consists in applying the Structure from Motion and Multi-View Stereo (SfM-MVS) workflow. From a set of overlapping images, SfM-MVS workflow produces high details 3D point clouds that can be derived in Digital Surface Models (DSM) and/or orthophotos. Few works were devoted to the 3D reconstruction of coastal structures using UAS-based imagery surveys. Based on our knowledge, the relevant studies focused on evaluating the capability of UAS to provide accurate geoinformation of coastal structures geometry (Gonçalves et al., 2022; González-Jorge et al., 2016; Henriques et al., 2014). Henriques et al., (2014) assessed the horizontal and vertical accuracy of DSM obtaining 10 cm and 8 cm respectively from a set of check points measured with a GNSS receiver. The potentiality of UAS surveys was confirmed by identifying sub-degree sensibility to armour units rotation (González-Jorge et al., 2016). Recently, Gonçalves et al., (2022) proved the advantage of UAS surveys when compared with Terrestrial Laser Scanning surveys in terms of fieldwork time and data completeness.

Among different environments, the vertical accuracy of DSM can be improved combining images with nadiral and oblique viewing angles (Manfreda et al., 2019). Broadly speaking, the accuracy of UAS products presents better horizontal than vertical accuracy

* Corresponding Author

(Rangel et al., 2018). The UAS with onboard Global Navigation Satellite System and Real Time Kinematics can avoid the use of GCPs by accurately estimate the images position (Taddia et al., 2019). However, the use of ground control points (GCP) in SfM-MVS workflow may improve the estimation of camera distortion parameters (Štroner et al., 2021).

The damage in coastal structures is expressed by indicators that characterize armour layer geometry. The most important ones are armour layer porosity and packing density (CIRIA et al., 2007). However, the damage percentage expressed by the fraction between the number of displaced armour units and the total number of armour units can also be used to identify likely damaged areas (Musumeci et al., 2018). Another approach may consider profiles transects to estimate the erosion areas over time (Melby and Kobayashi, 1998).

This work aims at validating the combination of UAS-RTK and SfM photogrammetry to reconstruct the geometry of rubble mound groins. From a UAS-based imagery network, the groin geometry was obtained through SfM-MVS and then, validated against the reference data collected with GNSS survey. We also discussed the contribution that UAS-RTK combined with SfM photogrammetry can provide to the traditional monitoring methods for assessing the structural integrity of armour layer.

2. STUDY SITE AND METHOD

This section describes the methodology to evaluate the geospatial information provided by an UAS survey on a rubble mound groin for armour layer monitoring. Firstly, we introduce the study site and characterize the surveys (section 2.1). Secondly, it is explained briefly the photogrammetric workflow in Agisoft Metashape to generate a 3D point cloud which is then derived in a DSM and an orthophoto (section 2.2). Finally, the accuracy assessment of vertical position is calculated through the linear regression adjustment and conventional root mean square error (section 2.3).

2.1 Study site and surveys

The study area is Leirosa Beach, located in the central zone of the Portuguese coastal zone, with NE-SW orientation (Figure 1). The groin has a L-shaped with an extension of 300 m and is composed of stone blocks of about 2.5 m and a mass of about 15 tonnes. The two groin heads show stone blocks displacements caused mainly by wave attacks.

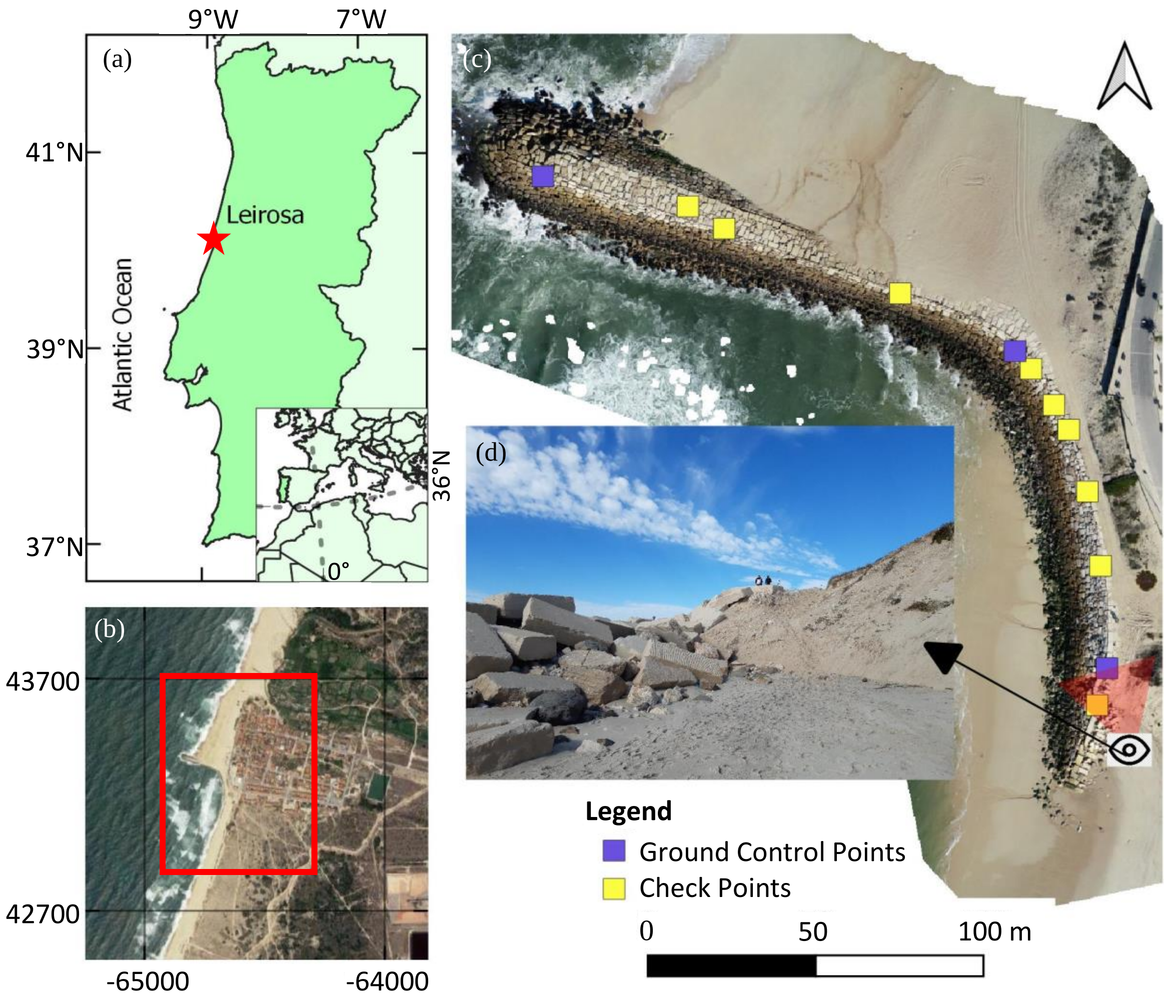

Figure 1. Study area illustration. (a and b) Location of Leirosa Beach in the Portuguese coast (red star in (a) and red rectangle in (b)). (c) Orthophoto generated by drone survey of Leirosa groin. The colorized squares represent the control points used in the photogrammetric process. (d) Photo of the south groin head showing several blocks displacements.

On 5th November 2021, a fieldwork campaign was conducted during low tide. The data was collected with a low-cost UAS DJI Phantom 4RTK (P4RTK) and a dual-frequency GNSS receiver Geomax Zenith 10. P4RTK is equipped with a 1'' CMOS sensor Sony FC6310 (20 Mpixels, a focal length of 8.8 mm and an image size of 5472×3648 pixels) and with onboard Global Navigation Satellite System and Real Time Kinematics.
The UAS survey was planned in DJI GST RTK software defining a regular grid path. A set of 103 nadiral images was collected at an altitude of 50 m for ensuring a Ground Sample Distance (GSD) with centimeter order (estimated mean GSD of 1.56 cm/pixel). We selected a side and front overlap of 80% to guarantee suitable image overlap for applying the photogrammetric workflow (section 2.2). In the end, the UAS survey lasted about 10 min.
From GNSS survey, it was measured a set of 54 points. 12 points were used as control points in the photogrammetric workflow (section 2.2). The remaining 42 points were used for a depth analysis of the vertical accuracy of DSM derived by the photogrammetric workflow (section 2.3).

2.2 Processing work

The images acquired with the P4RTK were processed using the SfM-MVS technique to obtain a 3D dense point cloud. The photogrammetric workflow was implemented in Agisoft Metashape and it is composed of four main steps (Gonçalves et al., 2021): (1) image alignment calculating the image external orientation parameters and the camera internal orientation parameter (IOP) through bundle adjustment; (2) tie points (correspondent point in zones of image overlap) refinement; (3) re-do bundle adjustment using the refined tie points; (4) dense matching applying MVS algorithms. Between steps 3 and 4, the control points were manually marked in images selecting 3 as GCP and 9 as check points (CHP) to evaluate the georeferencing of the resulting 3D dense point cloud (Figure 1c). Table 1 compiles the Agisoft Metashape workflow steps and the main values for each parameter used to generate the 3D dense point cloud.

Agisoft Metashape function	Parameter	Value
Align Photos	Generic Preselection	True
	Reference Preselection	Source
	Accuracy	True
	Tie points Limit	4000
	Key Point Limit	60000
	Adaptive camera model fitting	False
Gradual Selection	Reprojection Error	0.5
Optimize Cameras	IOP (f, cx, cy, k1, k2, k3, p1, p2)	NA
Build Dense Cloud	Quality	High
	Depth Filtering	Mild

Table 1. Agisoft Metashape processing parameters used in a typical photogrammetric workflow. NA - Not Applicable

Therefore, a Digital Surface Model (DSM) was generated from the 3D dense point cloud with a grid size of 5 cm choosing the interpolation of the empty grid cells. Finally, the image network was orthorectified to produce the orthophoto of the groin with a pixel size of 1.5 cm.

2.3 Accuracy assessment

The accuracy assessment aimed at evaluating the feasibility of UAS-based imagery to provide valid geospatial information of the groin surface. The points measured with the GNSS survey on the groin blocks were used to assess the vertical accuracy (Z_{GNSS}). Considering the planimetric position of profile points, the elevation of UAS (Z_{UAS}) was interpolated on the DSM.
The vertical deviation (d_Z) was therefore computed as

$$d_Z = Z_{GNSS} - Z_{UAS} \tag{1}$$

Firstly, linear regression was used to adjust the function that approximated the set of points composed by Z_{GNSS} (independent variable) and Z_{UAS} (dependent variable). Linear regression estimates the parameters m and b of the affine function

$$g(x)=mx+b \tag{2}$$

This adjustment can be assessed through the calculation of the determination coefficient (R). R can have values in a range of 0 (worst adjustment) and 1 (perfect adjustment).
Secondly, the vertical accuracy was also computed using the root mean square error (RMSE) of the deviations computed by Equation 1.

3. RESULTS

The photogrammetric workflow generated a high 3D dense point cloud with about 40 million points. The 3D dense point cloud was manually cropped particularly in the wave breaking zone to remove mismatches of SfM-MVS. The DSM covered the entire groin and the erosion and sediment retention zones (Figure 2a). In georeferencing process, we used 3 GCP resulting in a RMSE of 2.6 cm. The remaining 9 points were used as CHP resulting in a RMSE of 3.4 cm.
To further test, the set of Z_{GNSS} was divided into 1) profile points (P - 34 points) and 2) sample points along the west part of groin (CHP_Z - 8 points; Figure 2b). All profiles measured by GNSS survey were used to evaluate the vertical accuracy on the groin surface (Figure 2c). The profiles on DSM had a resolution of 50 cm contributing more details than the GNSS survey. Figure 3 shows a quantitative comparison between the vertical accuracy of Z_{GNSS} and Z_{UAS}. The histogram was plotted using a bin spacing of 1 cm. 50% of vertical deviation varied from -3.2 cm and -1.2 cm (interquartile range). Overall, the linear regression model returned a high agreement between Z_{GNSS} and Z_{UAS} (determination coefficient equal to 0.998). Regarding the deviations computed in RMSE, the vertical accuracy was found equal to 2.6 cm in P and 2.5 cm in CHP_Z. Finally, the weighted mean (based on point number) between P and CHP_Z was found approximately equal to 2.6 cm proving the stability of vertical accuracy over the DSM.

4. DISCUSSION

The present work demonstrates the potential of combining a Real-Time Kinematic assisted Unmanned Aerial System (UAS-RTK) and Structure from Motion (SfM) photogrammetry to reconstruct the geometry of rubble mound groins. The UAS-RTK survey provided a simple procedure with less fieldwork demanding when compared with other more accurate remote sensing techniques such as Terrestrial Laser Scanning (Gonçalves et al., 2022). The simplified Metashape workflow provided an easy-to-use implementation of SfM photogrammetry processing workflow to generate an accurate 3D dense point cloud (Gonçalves et al., 2021). Since the geometry of the image network was acquired only with nadiral images, the combination of nadiral and oblique images may improve mainly the vertical accuracy (Manfreda et al., 2019) and will be also beneficial to improve the density of the 3D dense point clouds (Rossi et al., 2017). Even though UAS-RTK does not require control points for the georeferencing process, we used 3 GCPs to ensure the

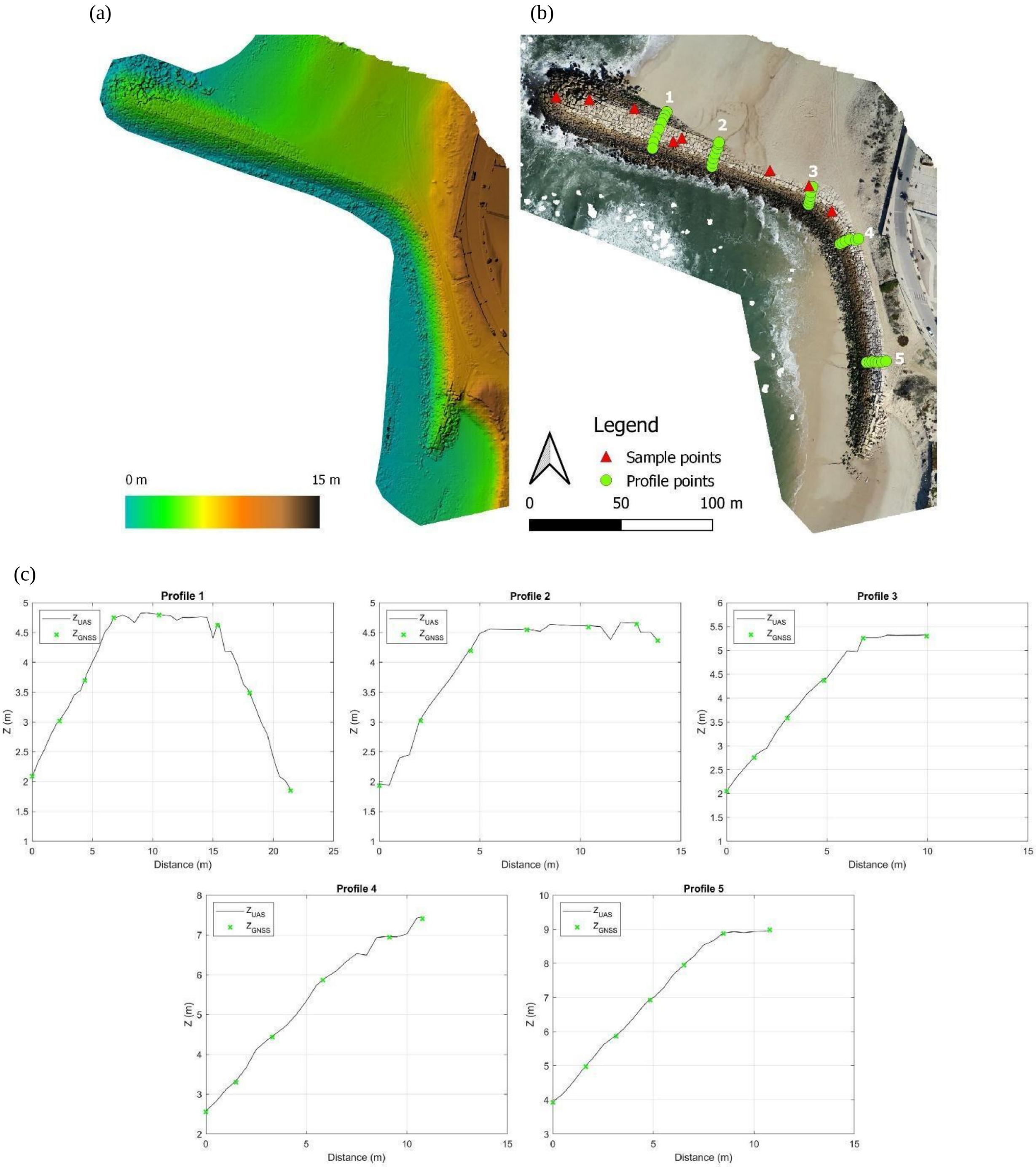

Figure 2. Products obtained DJI Phantom 4RTK and generated in Agisoft Metashape. (a) Digital Surface Model (DSM); (b) Orthophoto and the point used in vertical accuracy analysis. (c) The profiles were obtained with GNSS (green crosses) and UAS DSM (black lines with 50 cm bin spacing).

correction of camera internal orientation parameters (Štroner et al., 2021). A limitation of this accuracy analysis was the lack of sample points (CHP_Z) in the shore-parallel sector of the groin and in the likely damaged areas of the groin (mainly in heads - Figure 1).

Broadly speaking, the existing techniques for collecting geospatial data on the physical state of coastal structures are based on visual inspections that require qualified technicians. The use of UAS-RTK can provide a valuable alternative to improve the traditional monitoring methods. The resulting DSM provided high vertical accuracy of the groin surface. In fact, from the interpolation of the profiles and sample points, the results of vertical accuracy analysis returned a low Root Mean Square Error (RMSE – 2.6 cm). The use of UAS-RTK improved the vertical accuracy reported by Henriques et al. (2014) who obtained a RMSE of 8 cm. Overall, we showed that the DSM generated by the UAS-RTK survey can be used to implement monitoring methods for evaluating the structural condition of armour layer. For instance, it will possible to calculate the deformations of armour layer using cross-sections (Melby and Kobayashi, 1998). On the other hand, an in-depth investigation is required to calculate the indicators that characterize the armour layer geometry (e.g., packing density, armour layer porosity, and damage percentage). Due to the high spatial resolution of the orthophoto (1.5 cm/pixel), the automatic segmentation of block in orthophoto based on object-based image analysis (OBIA) (Cooper et al., 2021) can be a feasible option. Therefore, combining with the information provided by the DSM, it will be possible to isolate and measure horizontal and vertical movements of the armour unit.

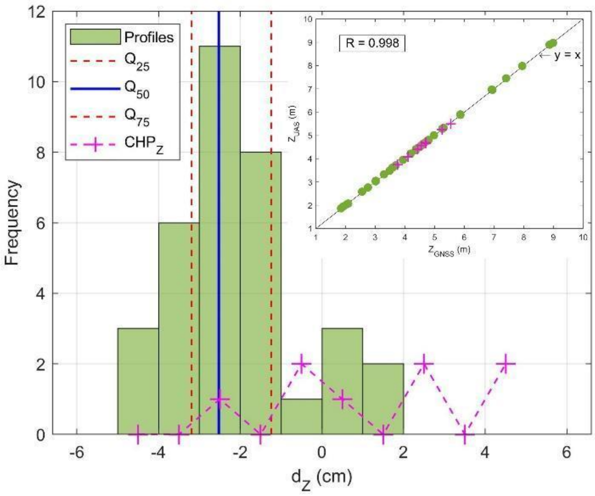

Figure 3. Differences in elevation between points measured in the GNSS survey and the elevation obtained UAS DSM. Q_{25}, Q_{50} and Q_{75} are the quartiles of deviations in profiles points. The plus-dash line illustrates the histogram of CHP_Z. In the top right is represented the linear regression of the vertical position. Circles correspond to P and plus sign correspond to CHP_Z.

5. CONCLUSION

This work showed the validation of Real-Time Kinematic assisted Unmanned Aerial Systems (UAS-RTK) surveys combined with Structure from Motion (SfM) photogrammetry to reconstruct the geometry of rouble mound groins for monitoring displacements in armour units.

The UAS-RTK survey allowed to map the entire groin including the areas hard-to-reach by the technicians. The flight was automatically planned and lasted about 10 min. The vertical accuracy of the Digital Surface Model (DSM), in comparison with the traditional GNSS, returned a RMSE of 2.6 cm. Therefore, the UAS-RTK DSM and orthophoto present an effective and accurate alternative to evaluate the geometry of rubble mound groins.

Future work will investigate the segmentation techniques of orthophotos based on Object-Based Image Analysis, in order to automatically isolate armour layer units to track vertical and horizontal movements. As result, it will be computed the main armour layer indicators (armour layer porosity and packing density) for assessing the integrity of the structure.

ACKNOWLEDGEMENTS

This work was supported by the Portuguese Foundation for Science and Technology (FCT) in the framework of UIDB/00308/2020 and the research project UAS4Litter (PTDC/EAM-REM/30324/2017). The work of D.G. was supported by the grant UI0308-D.Remota1/2020 funded by the Institute for Systems Engineering and Computers at Coimbra (INESC Coimbra) with the support of Portuguese Foundation for Science and Technology (FCT) through national funds (PIDDAC) in the framework of UIDB/00308/2020. MCC also acknowledges the support of CEMMPRE (project UID/EMS/00285/2020) by FCT/MCTES and, through national funds. The work of J.A. was supported by the Junta de Extremadura and European Regional Development Fund (ERDF) grant number GR18053 to the Research Group NEXUS (University of Extremadura).

REFERENCES

Andriolo, U., Almeida, L.P., Almar, R., 2018. Coupling terrestrial LiDAR and video imagery to perform 3D intertidal beach topography. *Coast. Eng.* 140, 232–239. https://doi.org/10.1016/j.coastaleng.2018.07.009

Andriolo, U., Gonçalves, G., Bessa, F., Sobral, P., 2020. Mapping marine litter on coastal dunes with unmanned aerial systems: A showcase on the Atlantic Coast. *Sci. Total Environ.* 736, 139632. https://doi.org/https://doi.org/10.1016/j.scitotenv.2020.139632

Andriolo, U., Gonçalves, G., Rangel-Buitrago, N., Paterni, M., Bessa, F., Gonçalves, L.M.S., Sobral, P., Bini, M., Duarte, D., Fontán-Bouzas, Á., Gonçalves, D., Kataoka, T., Luppichini, M., Pinto, L., Topouzelis, K., Vélez-Mendoza, A., Merlino, S., 2021. Drones for litter mapping: An inter-operator concordance test in marking beached items on aerial images. *Mar. Pollut. Bull.* 169, 112542. https://doi.org/10.1016/j.marpolbul.2021.112542

Bañón, L., Pagán, J.I., López, I., Banon, C., Aragonés, L., 2019. Validating UAS-based photogrammetry with traditional topographic methods for surveying dune ecosystems in the Spanish Mediterranean coast. *J. Mar. Sci. Eng.* 7. https://doi.org/10.3390/jmse7090297

Bush, D.M., Pilkey, O.H., Neal, W.J., 2001. *Encyclopedia of Ocean Sciences*, Second Edi. ed. Academic Press. https://doi.org/doi.org/10.1016/B978-012374473-9.00078-3

CIRIA, CUR, CETMEF, 2007. *The Rock Manual. The use of rock in hydraulic engineering*, 2 nd. ed. C683, CIRIA, London.

Cooper, H.M., Wasklewicz, T., Zhu, Z., Lewis, W., Lecompte, K., Heffentrager, M., Smaby, R., Brady, J., Howard, R., 2021. Evaluating the ability of multi-sensor techniques to capture topographic complexity. *Sensors* 21(6), 2105. https://doi.org/10.3390/s21062105

Duarte, D., Andriolo, U., Gonçalves, G., 2020. Addressing the Class Imbalance Problem in the Automatic Image Classification of Coastal Litter From Orthophotos Derived From UAS Imagery. *ISPRS Ann. Photogramm. Remote Sens. Spatial Inf. Sci*., V-3–2020, 439–445. https://doi.org/10.5194/isprs-annals-v-3-2020-439-2020

Gómez-Gutiérrez, Á., Gonçalves, G.R., 2020. Surveying coastal cliffs using two UAV platforms (multirotor and fixed-wing) and three different approaches for the estimation of volumetric changes. *Int. J. Remote Sens.* 41, 8143–8175. https://doi.org/10.1080/01431161.2020.1752950

Gonçalves, D., Gonçalves, G., Pérez-Alvárez, J.A., Andriolo, U., 2022. On the 3D Reconstruction of Coastal Structures by Unmanned Aerial Systems with Onboard Global Navigation Satellite System and Real-Time Kinematics and Terrestrial Laser Scanning. *Remote Sens.* 14(6), 1485. https://doi.org/https://doi.org/10.3390/rs14061485

Gonçalves, G., Gonçalves, D., Gómez-Gutiérrez, Á., Andriolo, U., Pérez-Alvárez, J.A., 2021. 3D Reconstruction of Coastal Cliffs from Fixed-Wing and Multi-Rotor UAS: Impact of SfM-MVS Processing Parameters, Image Redundancy and Acquisition *Geometry. Remote Sens.* 13(6), 1222. https://doi.org/https://doi.org/10.3390/rs13061222

González-Jorge, H., Puente, I., Roca, D., Martínez-Sánchez, J., Conde, B., Arias, P., 2016. UAV Photogrammetry Application to the Monitoring of Rubble Mound Breakwaters. *J. Perform. Constr. Facil.* 30, 04014194. https://doi.org/10.1061/(asce)cf.1943-5509.0000702

Henriques, M.J., Fonseca, A., Roque, D., Lima, J.N., Marnoto, J., 2014. Assessing the Quality of an UAV-based Orthomosaic and Surface Model of a Breakwater.

Henriques, M.J., Lemos, R., Capitão, R., Fortes, C.J., 2017. The monitoring of rubble mound breakwaters . An assessment of UAV technology. *INGEO 2017 – 7th Int. Conf. Eng. Surv*. 1–8.

Laporte-Fauret, Q., Lubac, B., Castelle, B., Michalet, R., Marieu, V., Bombrun, L., Launeau, P., Giraud, M., Normandin, C., Rosebery, D., 2020. Classification of Atlantic coastal sand dune vegetation using in situ, UAV, and airborne hyperspectral data. *Remote Sens.* 12. https://doi.org/10.3390/rs12142222

Mancini, F., Dubbini, M., Gattelli, M., Stecchi, F., Fabbri, S., Gabbianelli, G., 2013. Using unmanned aerial vehicles (UAV) for high-resolution reconstruction of topography: The structure from motion approach on coastal environments. *Remote Sens.* 5(12), 6880–6898. https://doi.org/10.3390/rs5126880

Manfreda, S., Dvorak, P., Mullerova, J., Herban, S., Vuono, P., Arranz Justel, J., Perks, M., 2019. Assessing the Accuracy of Digital Surface Models Derived from Optical Imagery Acquired with Unmanned Aerial Systems. *Drones* 3(1), 15. https://doi.org/10.3390/drones3010015

Medjkane, M., Maquaire, O., Costa, S., Roulland, T., Letortu, P., Fauchard, C., Antoine, R., Davidson, R., 2018. High-resolution monitoring of complex coastal morphology changes: cross-efficiency of SfM and TLS-based survey (Vaches-Noires cliffs, Normandy, France). *Landslides* 15, 1097–1108. https://doi.org/10.1007/s10346-017-0942-4

Melby, J.A., Kobayashi, N., 1998. Damage progression on breakwaters. *Proc. Coast. Eng. Conf.* 2, 1884–1897. https://doi.org/10.1061/9780784404119.141

Musumeci, R.E., Moltisanti, D., Foti, E., Battiato, S., Farinella, G.M., 2018. 3-D monitoring of rubble mound breakwater damages. *Meas. J. Int. Meas. Confed.* 117, 347–364. https://doi.org/10.1016/j.measurement.2017.12.020

Pagán, J.I., Bañón, L., López, I., Bañón, C., Aragonés, L., 2019. Monitoring the dune-beach system of Guardamar del Segura (Spain) using UAV, SfM and GIS techniques. *Sci. Total Environ.* 687, 1034–1045. https://doi.org/10.1016/j.scitotenv.2019.06.186

Rangel, J.M.G., Gonçalves, G., Pérez, J.A., 2018. The impact of number and spatial distribution of GCPs on the positional accuracy of geospatial products derived from low-cost UASs. *Int. J. Remote Sens.* 39, 7154–7171. https://doi.org/10.1080/01431161.2018.1515508

Rossi, P., Mancini, F., Dubbini, M., Mazzone, F., Capra, A., 2017. Combining nadir and oblique uav imagery to reconstruct quarry topography: Methodology and feasibility analysis. Eur. J. *Remote Sens.* 50, 211–221. https://doi.org/10.1080/22797254.2017.1313097

Rotnicka, J., Dłużewski, M., Dąbski, M., Rodzewicz, M., Włodarski, W., Zmarz, A., 2020. Accuracy of the UAV-Based DEM of Beach–Foredune Topography in Relation to Selected Morphometric Variables, Land Cover, and Multitemporal Sediment Budget. *Estuaries and Coasts* 43, 1939–1955. https://doi.org/10.1007/s12237-020-00752-x

Ružić, I., Marović, I., Benac, Č., Ilić, S., 2014. Coastal cliff geometry derived from structure-from-motion photogrammetry at Stara Baška, Krk Island, Croatia. *Geo-Marine Lett.* 34. https://doi.org/10.1007/s00367-014-0380-4

Štroner, M., Urban, R., Seidl, J., Reindl, T., Brouček, J., 2021. Photogrammetry Using UAV-Mounted GNSS RTK: Georeferencing Strategies without GCPs. *Remote Sens.* 13, 1336. https://doi.org/10.3390/rs13071336

Taddia, Y., Stecchi, F., Pellegrinelli, A., 2019. Using dji phantom 4 rtk drone for topographic mapping of coastal areas. *Int. Arch. Photogramm. Remote Sens. Spatial Inf. Sci.*, XLII-2/W13, 625–630. https://doi.org/10.5194/isprs-archives-XLII-2-W13-625-2019

Turner, I.L., Harley, M.D., Drummond, C.D., 2016. UAVs for coastal surveying. *Coast. Eng.* 114, 19–24. https://doi.org/10.1016/j.coastaleng.2016.03.011

Zimmerman, T., Jansen, K., Miller, J., 2020. Analysis of UAS flight altitude and ground control point parameters on DEM accuracy along a complex, developed coastline. *Remote Sens.* 12(14), 2305. https://doi.org/10.3390/rs12142305